

THE HUBBLE DIAGRAM OF TYPE IA SUPERNOVAE: EVIDENCE FOR A COSMOLOGICAL CONSTANT

6.1 Applications of the Luminosity Distance

The luminosity distance we have encountered in the previous lecture is used by observational cosmologists in two ways. The first, and the more common, is to assume a cosmological model which gives $d_L = f(z)$, and use:

$$F_{\text{obs}} = \frac{L}{4\pi d_L^2} \quad (6.1)$$

to deduce the luminosities L of objects at cosmological distances with observed fluxes F_{obs} . While the value of L of course depends on the set of cosmological parameters adopted, this may be of secondary importance in applications which involve comparative studies. An example is the determination of the luminosity function of galaxies, or quasars, at a particular redshift (provided of course that the same set of cosmological parameters is used for all the galaxies under scrutiny).

The *luminosity function* (LF) describes analytically the number of galaxies per unit volume with luminosity in the range $[L, L + dL]$. It is usually well represented by the product of a power law and exponential—the *Schechter function*—which takes the form:

$$\Phi(L)dL = \phi^* \left(\frac{L}{L^*} \right)^\alpha e^{-L/L^*} \frac{dL}{L^*}, \quad (6.2)$$

where the *faint end slope* α is a negative number, L^* is the *characteristic* (or *fiducial*) *luminosity*, and ϕ^* is the overall normalisation. Note that in this form the LF diverges at the faint end—that is, there must be a turn-over at the faint end for the overall number of galaxies to be finite. However, the luminosity-weighted LF, $L \cdot \Phi(L)$, does converge, provided the faint-end slope $\alpha > -2$. In the local universe, the LF of galaxies in visible light (in the V -band) is well-fitted by a Schechter function with typical parameters:

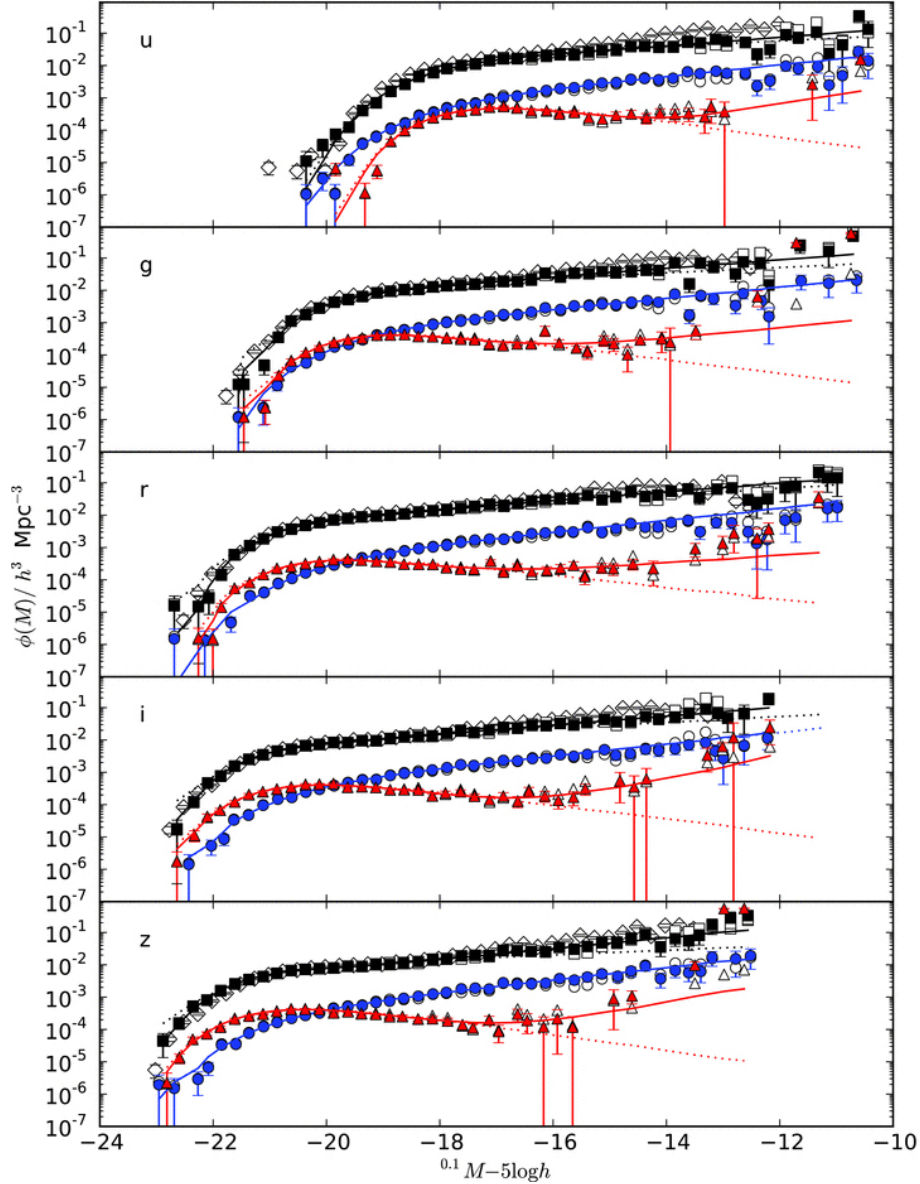


Figure 6.1: Luminosity functions of nearby galaxies ($z < 0.1$) published by the *Galaxy and Mass Assembly* (GAMA) project from data obtained with the Anglo-Australian telescope. The five panels refer to LFs in five different wavelength bands, from the ultraviolet, u, to the infrared, z. The LF is plotted separately for blue (i.e. star-forming) galaxies and red galaxies whose light is dominated by old stars. The black squares are for the combined blue and red samples. Dotted lines show the best fit to the data assuming a Schechter function (eq. 6.2). The GAMA team accumulated spectra of many thousands of galaxies to construct these LFs. (Reproduced from Loveday et al. 2012, MNRAS, 420, 1239).

$$\begin{aligned}
 \alpha &= -1.25 \\
 L^* &= 1.0 \times 10^{10} h^{-2} L_{\odot V} \\
 \phi^* &= 1.2 \times 10^{-2} h^3 \text{ Mpc}^{-3}
 \end{aligned}$$

In the past few years, it has become possible to extend studies of the galaxy luminosity function from the local Universe out to redshifts as high as $z \sim 8$ (see Fig. 6.2 as an example).

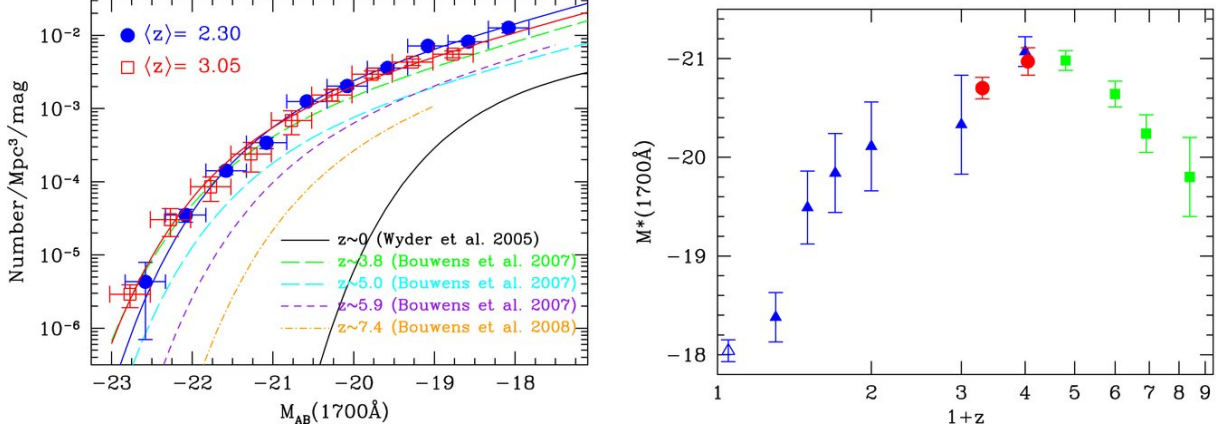


Figure 6.2: *Left*: Evolution of the ultraviolet (UV) luminosity function from $z = 7.4$ to $z = 0$. *Right*: Evolution of the characteristic UV luminosity (or absolute magnitude, M^* , at 1700 \AA) with redshift. (Reproduced from Reddy & Steidel 2009, ApJ, 692, 778).

The second use of the luminosity distance is the reverse of the first. Suppose we know the absolute luminosity of an astronomical source, then we could use its observed flux to deduce its luminosity distance from eq. 6.1. If we could be confident that the absolute luminosity is a constant in time and space, so that the object in question constitutes a *standard candle*, and if the source luminosity is sufficiently high that it can be detected over cosmological distances, then we could test for the cosmological parameters $\Omega_{m,0}$, $\Omega_{\Lambda,0}$, and $\Omega_{k,0}$ that determine the form of $d_L = f(z)$ according to the equations:

$$d_L(z) = \frac{c(1+z)}{\sqrt{|\Omega_{k,0}|}H_0} S_k \left(H_0 \sqrt{|\Omega_{k,0}|} \int_0^z \frac{dz}{H(z)} \right) \quad (6.3)$$

and

$$H(z) = H_0 \left[\Omega_{m,0} \cdot (1+z)^3 + \Omega_{k,0} \cdot (1+z)^2 + \Omega_{\Lambda,0} \right]^{1/2} = H_0 \cdot E(z)^{1/2} \quad (6.4)$$

Expressing the luminosity distance in terms of the distance modulus:

$$M - m = 2.5 \log \left(\frac{d_{L,0}}{d_L} \right)^2 = 5 \log \left(\frac{d_{L,0}}{d_L} \right), \quad (6.5)$$

where M is the magnitude of the standard candle at some nearby distance $d_{L,0}$. In the conventional definition of the distance modulus, $d_{L,0} = 10$ pc and M at this distance is usually referred to as the absolute magnitude. However, in cosmological situations this is a rather small distance and a more natural unit is 1 Mpc. If we measure the distance in this unit, the apparent magnitude is given by:

$$m = M + 5 \log d_L + 25. \quad (6.6)$$

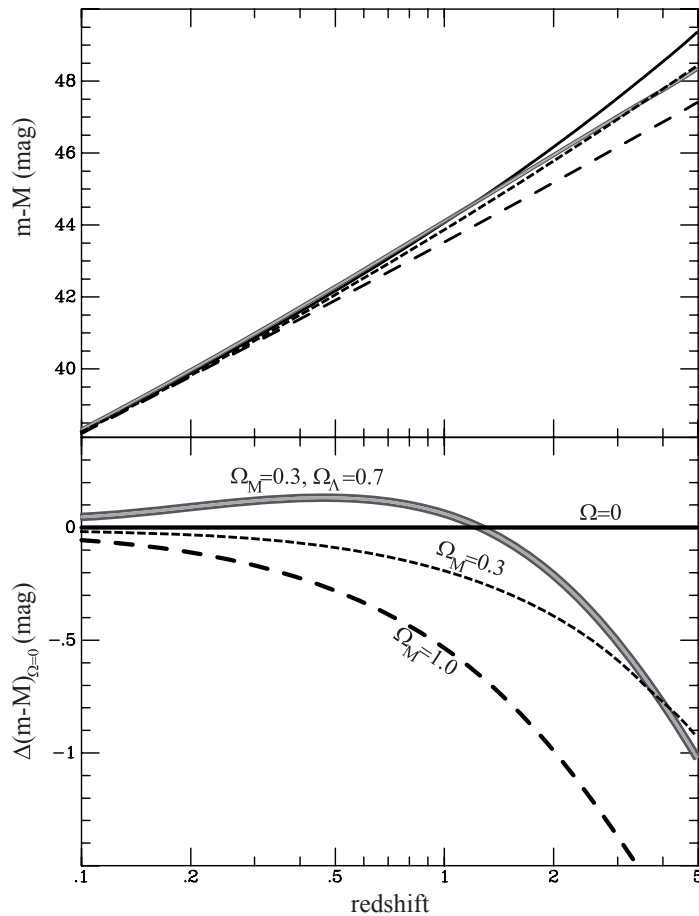


Figure 6.3: The distance modulus as a function of redshift for four relevant cosmological models, as indicated. In the lower panel the empty universe ($\Omega_{m,0} = \Omega_{\Lambda,0} = 0$) has been subtracted from the other models to highlight the differences.

Figure 6.3 illustrates the dependence of the distance modulus on redshift for four different sets of cosmological parameters. It can be seen that if we could measure the distance modulus of a standard candle with a precision of about 10%, or 0.1 magnitudes, out to redshifts $z > 0.5$, we may be able to distinguish a Λ -dominated universe from a matter-dominated one.

Incidentally, we can *measure* the absolute magnitude M , independently of Ω_i , in the local universe using the approximation for d_L we derived for small values of z (eq. 5.46):

$$d_L = (1+z)r_1 \approx \frac{c}{H_0} \left[z + \frac{1}{2}(1-q_0)z^2 + \dots \right]$$

to give:

$$m = M - 5 \log H_0 + 5 \log cz + \dots + 25. \quad (6.7)$$

A well-known example of standard candles are Cepheids, a class of variable stars which exhibit a period-luminosity relation which has allowed the determination of H_0 . However, Cepheids are intrinsically too faint to be followed beyond the local Universe. The class of astronomical objects which has so far turned out to be the closest approximation to a cosmological standard candle are the so-called type Ia supernovae.

6.2 Type Ia Supernovae

As early as 1938, Baade and Zwicky pointed out that supernovae were promising candidates for measuring the cosmic expansion. Their peak brightness seemed quite uniform, and they were bright enough to be seen at extremely large distances. In fact a supernova can, for a few weeks, be as bright as an entire galaxy [see Figure 6.4; SN 1998aq in NGC 3982 at a distance of ~ 20 Mpc reached peak magnitude $m_V = 11.4$, brighter than the whole galaxy which has $m_V = 11.8$]. Over the years, however, as more and more supernovae were measured, it became clear that they are in fact a heterogeneous group with a wide range of spectral characteristics and intrinsic peak brightnesses.

As as often the case in astronomy, the original classification of SNe into two types, type I and type II, was based on morphological characteristics—in this case of their spectra, rather than on physical understanding: type I and II supernovae were so classified simply on the basis of whether their spectra included any emission/absorption lines from neutral hydrogen. In the early 1980s a new subclassification of supernovae emerged: SNe of type I were further divided into type Ia and type Ib depending on the presence

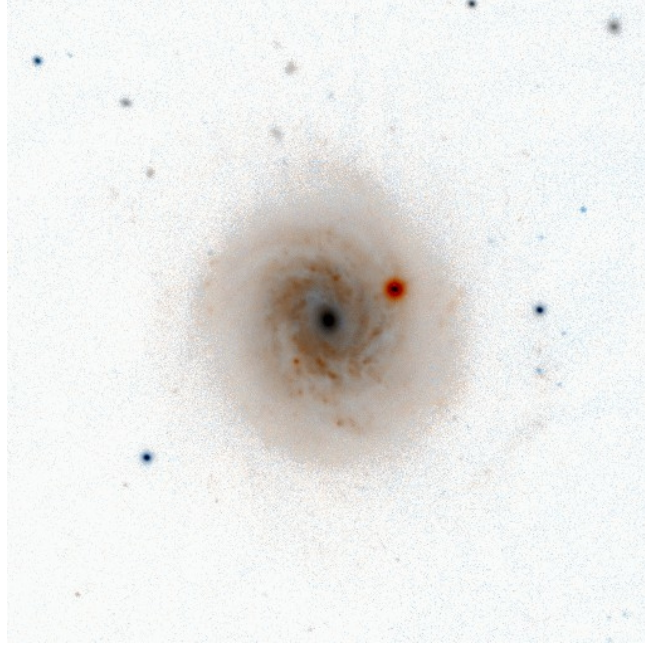


Figure 6.4: SN 1998aq in NGC 3982. This prototypical Type Ia supernova was discovered on 1998 April 13 by Mark Armstrong as part of the UK Nova/Supernova Patrol approximately two weeks before it reached its peak luminosity in the B -band. Its host galaxy, NGC 3982, is a nearly face-on spiral with a Seyfert 2 active nucleus. At a distance of 20.5 Mpc, NGC 3982 is a possible member of the Ursa Major cluster of galaxies.

or absence of a broad Silicon absorption feature at 6150 \AA in their red spectrum. It was soon realised that type Ia SNe exhibit a great uniformity not only in their spectral characteristics but also in their light curves—that is in the way their luminosity varies as a function of time, as they first brighten to a peak and then fade over a period of weeks.

Current thinking is that both type II and type Ib are core-collapse supernovae whose progenitors are massive stars, with $M > 8M_{\odot}$. They are the source of $\sim 90\%$ of the oxygen that we breathe.

SNe of type Ia are thought to be nuclear explosions of carbon/oxygen white dwarfs in binary systems (see Figure 6.5). The white dwarf (a stellar remnant supported by the degenerate pressure of electrons) accretes matter from an evolving companion and its mass increases toward the Chandrasekhar limit of $1.44 M_{\odot}$ (this is the mass above which the degenerate electrons become relativistic and the white dwarf unstable). Near this limit there is a nuclear detonation in the core in which carbon (or oxygen) is converted to iron. (Approximately two thirds of the iron in our haemoglobin was synthesised by type Ia SNe). A nuclear flame propa-

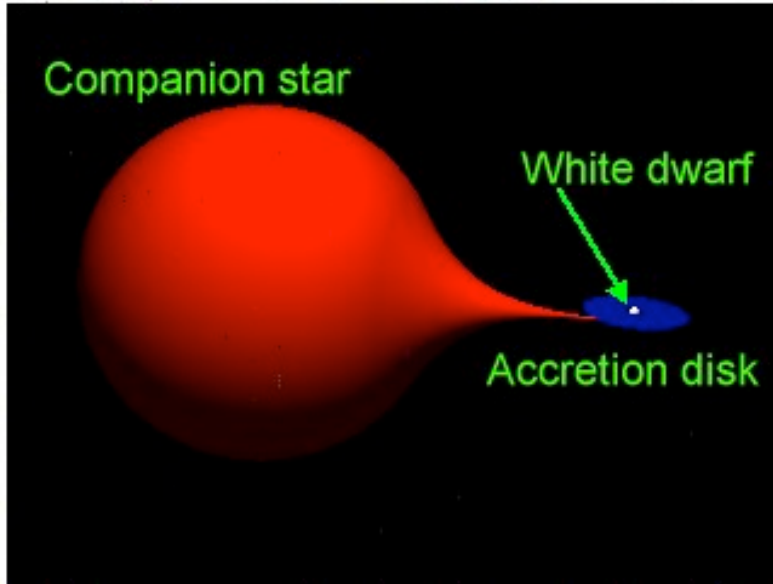


Figure 6.5: Schematic representation of the stellar progenitor of a Type Ia supernova.

gates to the exterior and blows the white dwarf apart (there are alternative models but this is the favoured scenario).

SNe of type Ia are seen in both young and old stellar populations; for example, they are observed in the spiral arms of spiral galaxies where there is active star formation at present, as well as in elliptical galaxies where vigorous star formation apparently ceased many Gyr ago. Locally, there appears to be no difference in the properties of SNIa arising in these two different populations, which is important because at large redshift the stellar population is certainly younger.

The value of SNIa as cosmological probes arises from the high peak luminosity as well as the observational evidence (locally) that this peak luminosity is the sought-after standard candle. In fact, the absolute magnitude, at peak, varies by about 0.5 magnitudes which corresponds to a 50%-60% variation in luminosity; this, on the face of it, would make them fairly useless as standard candles. However, the peak luminosity appears to be well-correlated with decay time: the larger L_{peak} , the slower the decay (see Figure 6.6). There are various ways of quantifying this effect, such as:

$$M_B \approx 0.8(\Delta m_{15} - 1.1) - 19.5, \quad (6.8)$$

where M_B is the peak absolute magnitude in the B -band and Δm_{15} is the observed change in apparent magnitude 15 days after the peak. This

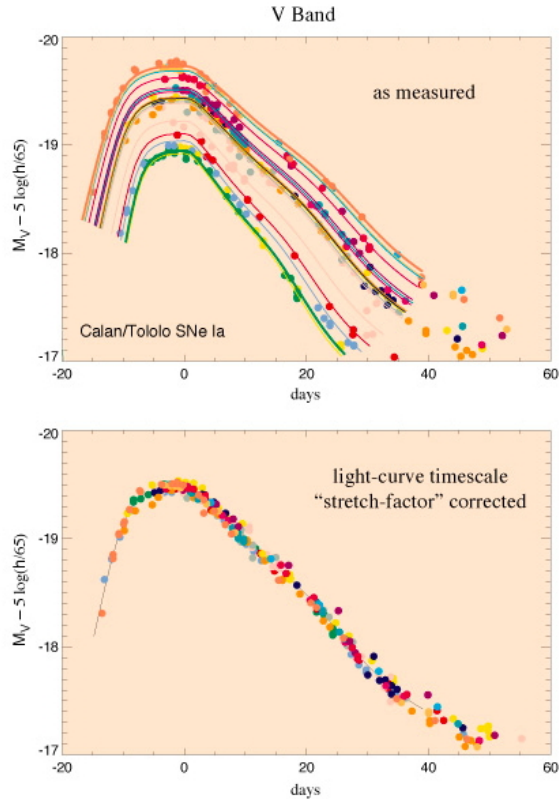


Figure 6.6: Light curves of type Ia SN before (*top*) and after (*bottom*) application of the correction of eq. 6.8. (Reproduced from <http://supernova.lbl.gov>).

is an empirical relationship, and there is no consensus about the theoretical explanation.¹ However, when this correction is applied it appears that $\Delta L_{peak} < 20\%$. If true, this means that SNIa are candles that are standard enough to distinguish between cosmological models at $z \approx 0.5$ (see Fig. 6.3).

In a given galaxy, supernovae are rare events (on a human time scale, that is), with one or two such explosions per century. But if thousands of galaxies can be surveyed on a regular and frequent basis, then it is possible to observe many events per year over a range of redshift. About 20 years ago two large international collaborations, the ‘*Supernova Cosmology Project*’, based at Berkeley, California, and the ‘*High-Z Supernova Search*’ based in Australia, Chile and Baltimore, Maryland, began such ambitious programs. Observations with the *Hubble Space Telescope* have proved crucial for following SN beyond $z \sim 0.5$ (see Figure 6.7). These efforts turned out

¹The existence of a well-defined mass threshold, $1.44 M_{\odot}$ for an accreting white dwarf to explode as a type Ia supernova is presumably at the root of this remarkable uniformity in their spectra and light curves, and the small residual degree of variation may reflect differences in accretion rates, rotational velocities and C/O ratios.

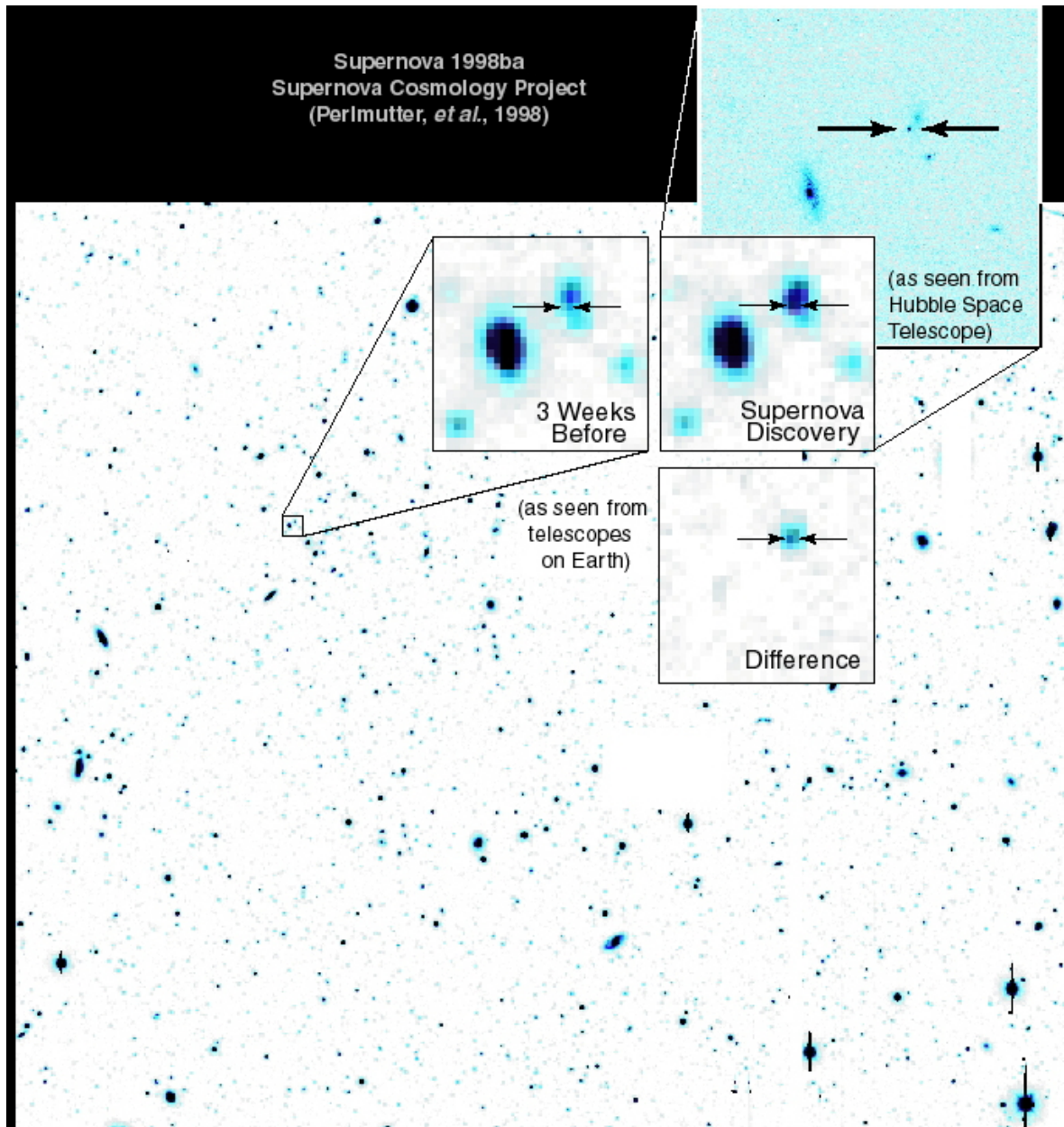


Figure 6.7: The superb resolution of the *Hubble Space Telescope* allows a more accurate measurement of the light curves of high redshift supernovae than is possible from the ground.

to be fruitful beyond the most optimistic expectations and the results led to a major paradigm shift in cosmology.

Fig. 6.8 shows the Hubble diagram for SNe of type Ia observed by the Supernova Cosmology Project up to 2003—the highest redshift supernova observed at that time was at $z = 0.86$. The conclusion seems to be that SNIa are 10% to 20% fainter at $z \approx 0.5$ than would be expected in an

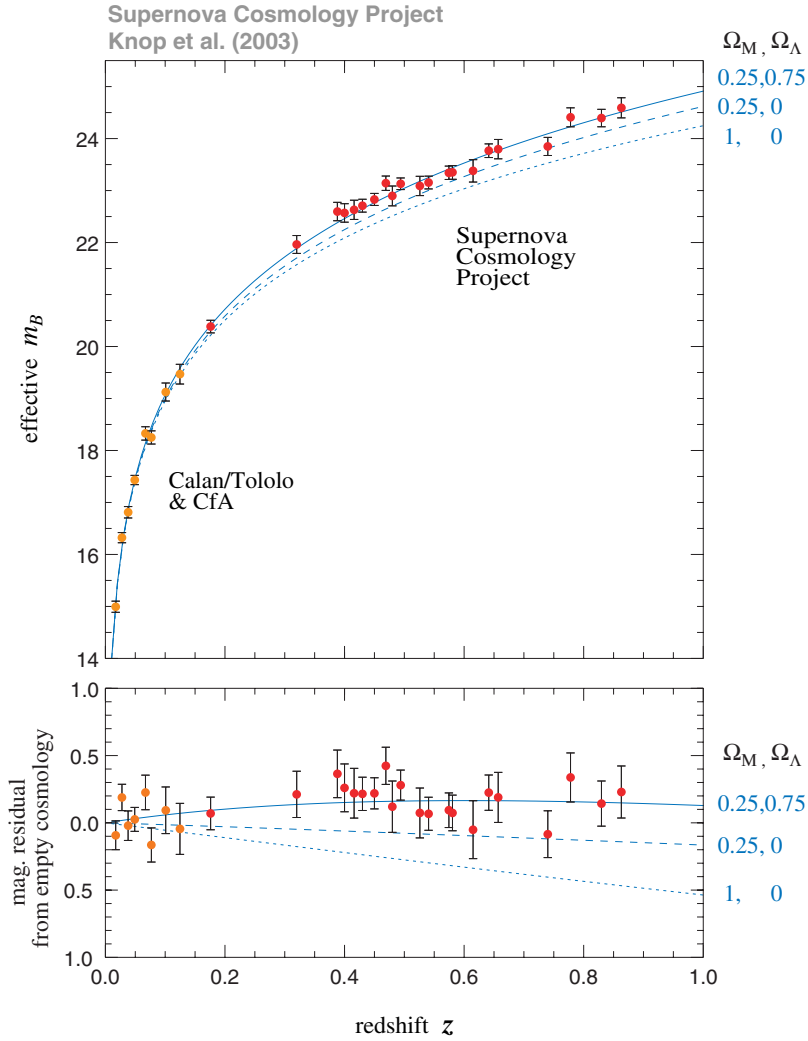


Figure 6.8: Hubble diagram for SNe Ia up to $z = 0.86$, reproduced from Knop et al. 2003, ApJ, 598, 102. The observed B -band magnitudes of the SNe Ia at maximum light are compared with the predictions for three cosmological models, as indicated. The lower panel shows the difference relative to an empty universe with $\Omega_{m,0} = \Omega_{\Lambda,0} = 0$ and $\Omega_{k,0} = 1$.

empty universe ($\Omega_{m,0} = \Omega_{\Lambda,0} = 0$ and $\Omega_{k,0} = 1$) and, more significantly, about 30% to 40% fainter than a model with $\Omega_{m,0} = 0.25$ (indicated by other considerations) and $\Omega_{\Lambda,0} = 0$. The introduction of a cosmological constant at the level $\Omega_{\Lambda,0} \simeq 0.75$ improves the fit to the SN magnitude vs. redshift relation significantly. The two teams concluded that we live in an accelerating universe (recall eq. 5.44 for the q_0 parameter), a discovery which *Science* magazine hailed as the “*The Breakthrough of the Year*”, and for which the leaders of the two teams were awarded the Nobel prize in physics in 2011 (as well as many other prestigious prizes).

6.2.1 Parameter Estimation

In this section we consider more closely the methods employed to determine the values of Ω_i which best fit the SN data shown in Fig. 6.8. The approach to this ‘parameter estimation problem’ has many applications in the analysis of scientific measurements.

Let us assume that we have a sample of n SN measurements consisting of magnitude m_i , typical magnitude error $\pm\sigma_{m,i}$, and redshift z_i (there is also an error associated with z_i , but it can be neglected, for our purposes, compared with $\sigma_{m,i}$). We wish to compare quantitatively this data set with theoretical expectations from Eqs. 6.6, 6.3 and 6.4 for different combinations of the parameters $(\Omega_{m,0}, \Omega_{\Lambda,0}, M)$.

There are two ways to tackle the absolute magnitude M . We could assume that we know M with sufficient precision from measurements of nearby SNaE via eq. 6.7 which, remember, does not depend on any value of Ω , but only on the Hubble constant H_0 (and the assumption of negligible peculiar velocities relative to the Hubble flow). Alternatively, we could consider M to be a free parameter alongside $\Omega_{m,0}$ and $\Omega_{\Lambda,0}$, and fit simultaneously for all three.

We’ll consider the second approach. In order to get a compact notation, we define the parameter vector:

$$\theta \equiv (\Omega_{m,0}, \Omega_{\Lambda,0}, M). \quad (6.9)$$

If we assume that the errors in the magnitude, $\sigma_{m,i}$ are purely of a random nature and are drawn from a Gaussian distribution², then we can obtain the best fit parameters by maximising the posterior probability (likelihood):

$$L(\theta) \propto \exp\left[-\frac{1}{2}\chi^2\right] \quad (6.10)$$

with

$$\chi^2 = \sum_{i=1}^n \left(\frac{m(z_i; \theta) - m_i}{\sigma_{m,i}}\right)^2 \quad (6.11)$$

²In scientific analysis this is often a crucial assumption, in the sense that generally we do not know all the sources of error in a measurement, random and systematic.

It is then relatively straightforward to minimise eq. 6.11 to obtain the best-fit value of θ . More importantly, by calculating the value of $L(\theta)$ over a whole region in parameter space—which is relatively straightforward to do with numerical techniques—we can generate the full distribution of probabilities for the set of parameters considered.

If we are most interested in the cosmological parameters $\Omega_{m,0}$ and $\Omega_{\Lambda,0}$, and less concerned with the value of M , we can marginalize over the absolute magnitude and restrict ourselves to the two-dimensional probability distribution

$$L(\Omega_{m,0}, \Omega_{\Lambda,0}) = \int dM L(\Omega_{m,0}, \Omega_{\Lambda,0}, M) \quad (6.12)$$

Figure 6.9 shows contours of $L(\Omega_{m,0}, \Omega_{\Lambda,0})$ at the 68%, 90%, 95%, and 99% levels on the $\Omega_{m,0} - \Omega_{\Lambda,0}$ plane for the SN data in Figure 6.8. Clearly a range of $\Omega_{m,0}, \Omega_{\Lambda,0}$ combinations can reproduce the SNIa peak magnitudes, but it is noteworthy that at the 95% confidence level we do require $\Omega_{\Lambda,0} > 0$.

The confidence contours on the $\Omega_{m,0} - \Omega_{\Lambda,0}$ plane are stretched along a

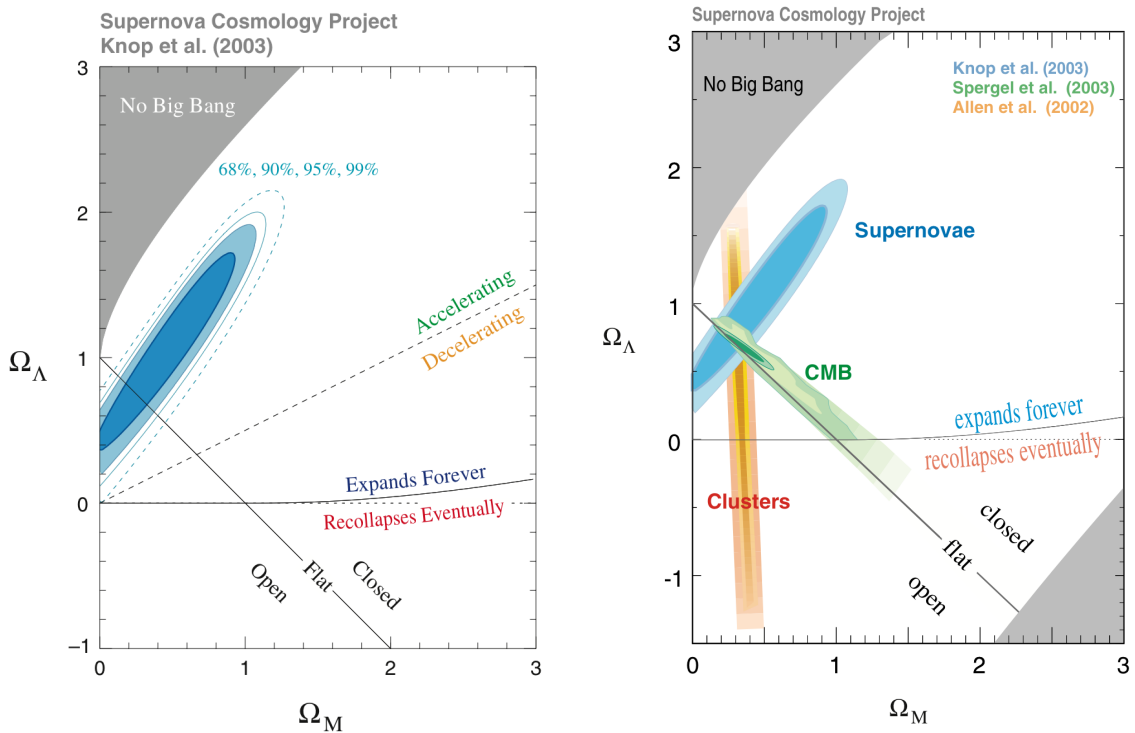


Figure 6.9: *Left:* Likelihood contours in the $\Omega_{m,0} - \Omega_{\Lambda,0}$ plane for the SN data in Figure 6.8. *Right:* Joint likelihood contours in the $\Omega_{m,0} - \Omega_{\Lambda,0}$ plane from type Ia supernovae, the angular power spectrum of the cosmic background radiation, and massive galaxy clusters.

line $\Omega_{\Lambda,0} = 1.4\Omega_{m,0} + 0.4$. Some other cosmological test, which depends on Ω_i in a different way from the luminosity distance, is thus required to narrow down the allowed region. The angular diameter distance test on the temperature fluctuations of the CMB on the sky—already mentioned in lecture 5—provides the most stringent of such constraints. The position of the first peak in the angular power spectrum (see Figure 5.7.), together with the amplitudes of the first two peaks, define a line on the $\Omega_{m,0} - \Omega_{\Lambda,0}$ plane which is nearly perpendicular to that of the SNIa measurements, at $\Omega_{m,0} + \Omega_{\Lambda,0} \simeq 1$, indicating that we live in a near-flat universe with $\Omega_{k,0} \simeq 0$. When we combine the CMB, SNIa and other measurements we arrive at today’s consensus cosmology with $\Omega_{m,0} \simeq 0.3$, $\Omega_{\Lambda,0} \simeq 0.7$, $\Omega_{k,0} \simeq 0$ (see Fig. 6.9).

Figure 6.10 shows updated versions of these likelihood contours constructed from a recent compilation of 580 SNe (the Union2.1 compilation).

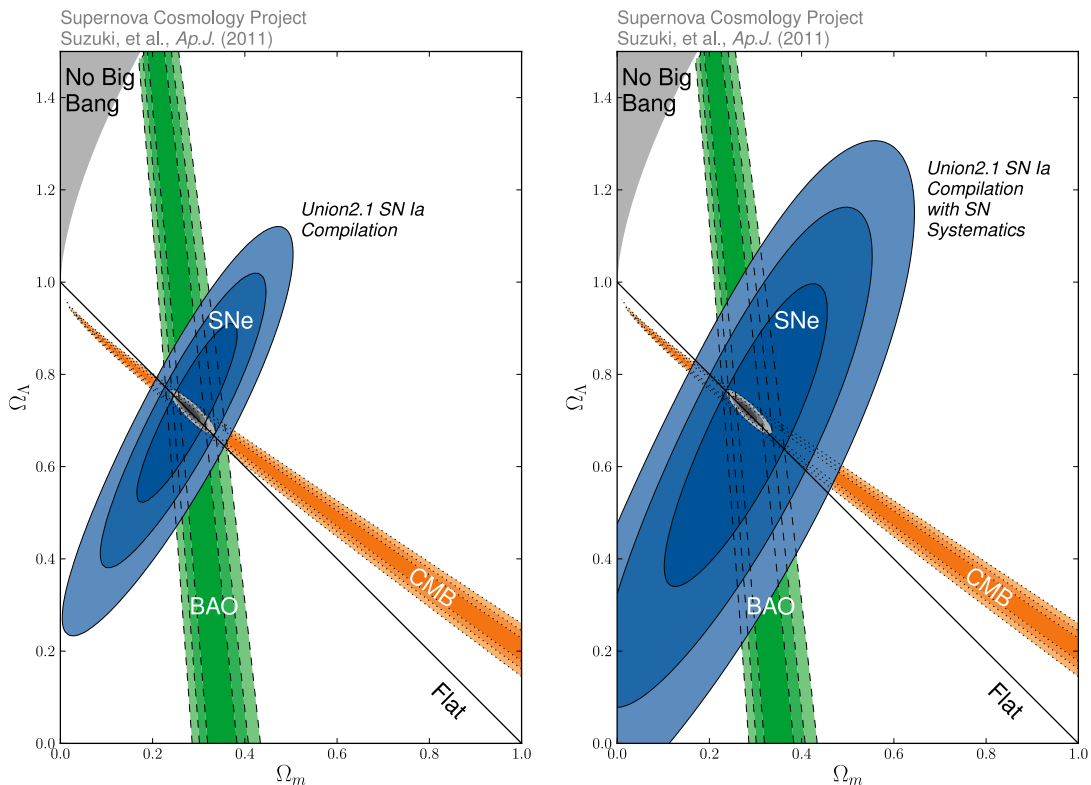


Figure 6.10: *Left*: Joint likelihood contours (68%, 95%, and 99.7% confidence limits) in the $\Omega_{m,0} - \Omega_{\Lambda,0}$ plane for a recent compilation of SN Ia data, together with the WMAP measure of the temperature anisotropies of the CMB, and the large-scale distribution of galaxies in the nearby Universe (BAO). *Right*: Same as left figure, but including systematic uncertainties in the SN Ia luminosity.

6.3 Alternative Explanations?

The evidence for a cosmological constant rests heavily on photometric measurement of distant sources that are found to be a few tenths of magnitude fainter than expected in the absence of a cosmological constant. Is this sufficient evidence for re-instating Einstein's 'Biggest Blunder' and open the door to a 'Dark Energy' of a totally unknown nature? Let's consider what other astrophysical effects may be producing the dimming of the supernovae maximum light.

1. **Evolution.** The whole edifice rests upon an empirical peak luminosity-decay rate relationship and, of course, upon the assumption that this relation does not evolve with look-back time. Is it possible that the properties of SNIa events may have evolved with cosmic time? The SN exploding at high redshift come from a systematically younger stellar population than the objects observed locally. Moreover, the abundances of carbon and oxygen may have been lower then; this evolving composition, by changing the opacity in the outer layers or the composition of the fuel itself could lead to a systematic evolution in peak luminosity. Here it is important to look for observational differences between local and distant supernovae—so far, there seem to be no significant differences in most respects, in either their spectra nor the light curves.
2. **Interstellar Dust.** It might be that supernovae in distant galaxies are more (or less) dimmed by dust than local supernovae. But normal dust, with particle sizes comparable to the wavelength of light, not only dims but also reddens the light of a background source. Thus, by comparing the colours of nearby and distant SNe, it should be possible to assess the importance of this effect. The upshot is that there seems to be no difference in the reddening of local and distant supernovae, implying that the distant events are not more or less obscured than the local ones.
3. **Grey Dust.** It is conceivable (but unlikely) that intergalactic space contains dust particles which are significantly larger than the wavelength of light. Such particles would dim but not redden the distant supernovae and so would be undetectable by the method described above. Contrived? Certainly, but so is Λ !

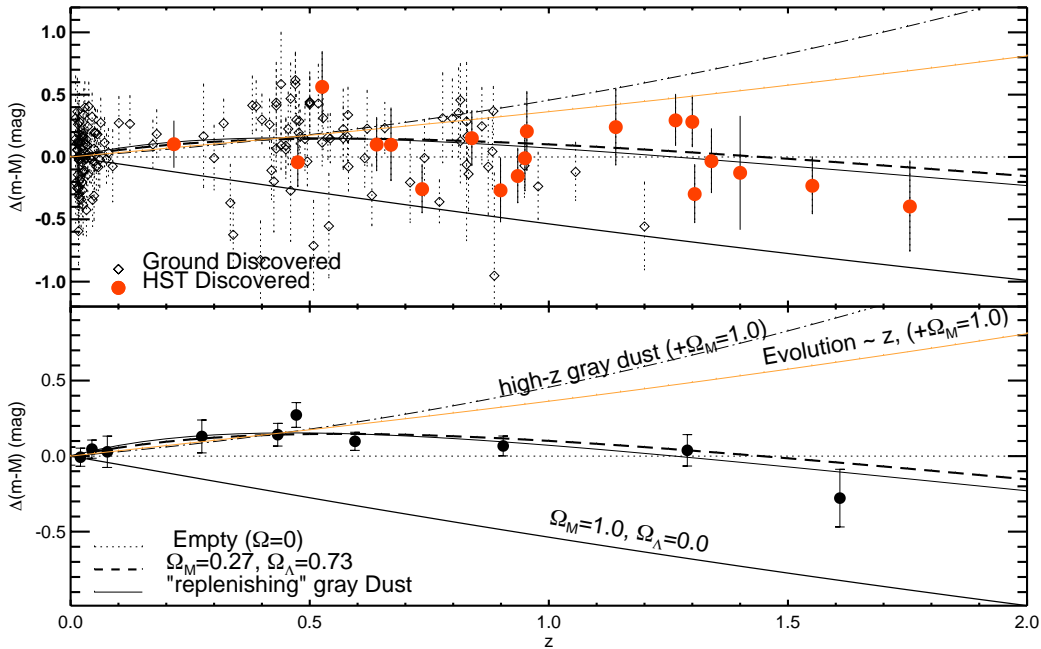


Figure 6.11: SNIa residual Hubble diagram comparing cosmological models and models with astrophysical dimming (reproduced from Riess et al. 2004, ApJ, 607, 665). Data and models are shown relative to an empty universe model ($\Omega_{m,0} = \Omega_{\Lambda,0} = 0$).

An empirical way to assess the validity of these alternative explanations is to push the measurement of SN Ia light curves to redshifts $z > 1$. A natural prediction of interpretations appealing to redshift evolution in the supernova properties and/or the presence of intergalactic grey dust (or any other explanation which we may label ‘astrophysical dimming’, as opposed to cosmological dimming), is that the dimming should continue, and possibly increase, with increasing look-back time. In contrast, a cosmological constant would lead to the SNe getting *brighter* again with increasing redshift beyond $z \sim 1$, because this is the epoch when the Λ term in the Friedmann equation (e.g. in the form given in eq. 4.10)

$$\dot{a}^2 = H_0^2 \Omega_{m,0} a^{-1} + H_0^2 \Omega_{\Lambda,0} a^2 \quad (6.13)$$

begins to become comparable to the matter term (see also Fig. 6.3)

After the initial reports indicating that we live in a Λ -dominated Universe, both supernova teams put the *Hubble Space Telescope* to work to extend their observations to $z > 1$. It was found that the behaviour of the distance modulus with z is indeed as expected in a cosmology with $\Omega_{m,0} \simeq 0.3$, $\Omega_{\Lambda,0} \simeq 0.7$ (see Figure 6.11). Models appealing to astrophysical dimming have to be so contrived that they are now considered very unlikely.

6.4 Dark Energy

In lecture 4 we associated an energy density with the cosmological constant

$$\rho_\Lambda \equiv \frac{\Lambda}{8\pi G} = \text{constant} \quad (6.14)$$

(adopting ‘natural units’, where $c = 1$, which we are going to maintain here). Recalling the fluid equation:

$$\dot{\rho} = -3(\rho + p)\frac{\dot{a}}{a} \quad (6.15)$$

which we first encountered as eq. 2.14, we see that for Λ :

$$p_\Lambda = -\rho_\Lambda . \quad (6.16)$$

That is, the cosmological constant can be viewed as another fluid component of the universe, like matter or radiation, but with a *negative* pressure. In simple fluids, pressure and density are related by the equation of state:

$$p_i = w_i \rho_i , \quad (6.17)$$

where w_i is a constant. From the point of view of cosmology, the relevant feature of each component is how its energy density evolves as the Universe expands. For fluids with an equation of state of the form given in 6.17, we have from eq. 6.15

$$\frac{\dot{\rho}_i}{\rho_i} = -3(1 + w_i)\frac{\dot{a}}{a} \quad (6.18)$$

so that the energy density has a power-law dependence on the scale factor:

$$\rho_i \propto a^{-n_i} , \quad (6.19)$$

where:

$$n_i = 3(1 + w_i) . \quad (6.20)$$

Our definition of the density parameter:

$$\Omega_i \equiv \frac{\rho_i}{\rho_{\text{crit}}} = \left(\frac{8\pi G}{3H^2} \right) \rho_i , \quad (6.21)$$

then has the useful property that:

$$\frac{\Omega_i}{\Omega_j} \propto a^{-(n_i - n_j)} . \quad (6.22)$$

Reviewing the components already discussed in lecture 2:

- Dust (a set of massive particles with negligible relative velocities, the component which we have called matter in the preceding lectures) has zero pressure, and an energy density which evolves as $\rho_M \propto a^{-3}$. Thus, for dust, $w = 0$.
- Radiation (any relativistic particle, not only photons) has an energy density that evolves as $\rho_R \propto a^{-4}$. Thus, for radiation, $w = 1/3$.
- The cosmological constant defined as in eq. 6.14 has an energy density which does not change as the universe expands, so that $\rho_\Lambda \propto a^0$. Thus, for the cosmological constant, $w = -1$.
- Curvature. With our definition (eq. 4.7)

$$\Omega_k \equiv -k/(aH)^2 \quad (6.23)$$

we can associate an effective ‘energy density in curvature’:

$$\rho_k = -\frac{3}{8\pi G} \frac{k}{a^2} \quad (6.24)$$

which varies as $\rho_k \propto a^{-2}$, so that for curvature $w = -1/3$.

We can now write for the expansion:

$$H(a) = H_0 \left(\sum_i \Omega_{i,0} a^{-n_i} \right)^{1/2} \quad (6.25)$$

The most popular equations of state for cosmological energy sources can be summarized as follows:

	w_i	n_i	
matter	0	3	
radiation	1/3	4	
‘curvature’	-1/3	2	
vacuum	-1	0	(6.26)

From our earlier definition of the deceleration parameter:

$$q(t) = -\frac{1}{H^2} \frac{\ddot{a}}{a} = -a \frac{\ddot{a}}{\dot{a}^2} \quad (6.27)$$

we now see that :

$$q = \sum_i \frac{n_i - 2}{2} \Omega_i \quad (6.28)$$

so that positive-energy-density sources with $n > 2$ cause the universe to decelerate ($q > 0$), while $n < 2$ leads to acceleration ($q < 0$). The more rapidly energy density redshifts away, the greater the tendency towards universal deceleration. An empty universe ($\Omega_m = \Omega_{\text{rad}} = \Omega_\Lambda = 0, \Omega_k = 1$) expands linearly with time. By considering eqs. 6.26 and 6.22 we can also immediately see that the cosmological constant comes to dominate over the energy density of other components at late times.

The database of SNIa measurements has been increasing significantly since their value for cosmology, as well as stellar evolution, has been appreciated. With improved statistics and more careful assessment of the many sources of systematic error, it has become possible to test whether the acceleration is indeed caused by a cosmological constant with $w = -1$, the vacuum energy of Einstein's equations, or another fluid component with a value of $n \neq 0$, but still satisfying the requirement of a negative q_0 when combined with the other components of our Universe according to eq. 6.28. A value

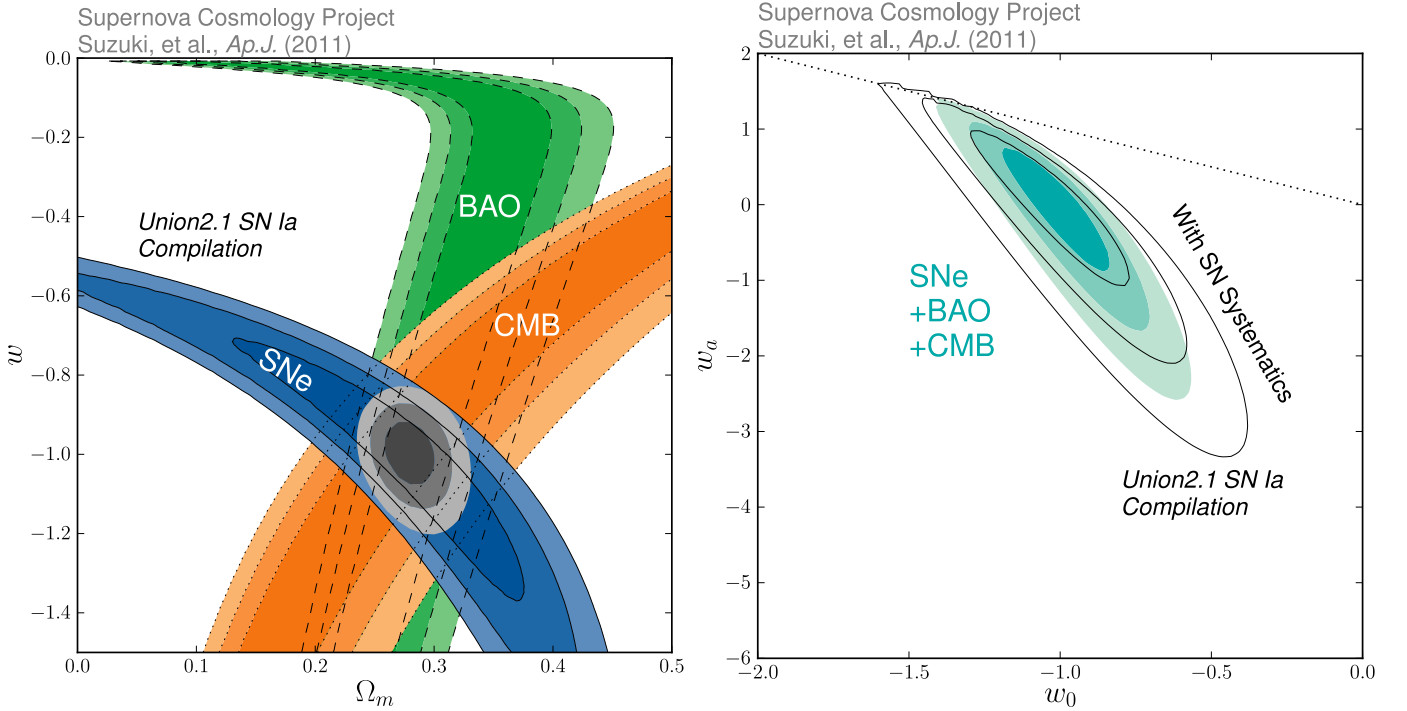


Figure 6.12: *Left*: Joint likelihood contours (68%, 95%, and 99.7% confidence limits) for $\Omega_{m,0}$ and the parameter w in the equation of state of dark energy. *Right*: Joint confidence contours between the parameters w_0 and w_a in eq. 6.29.

$w = -1$ is favoured by the current data; in their review, Weinberg et al. (2013, *Physics Reports* 530, 87-255—yes, this review is 169 pages long!) deduce $w = -1.007 \pm 0.081$ (see Figure 6.12).

Given how little we know about ‘dark energy’, may it not be possible that the parameter w is not constant in time, but rather evolves linearly (in the simplest case) with the scale factor according to:

$$w(a) = w_0 + w_a(1 - a) ? \tag{6.29}$$

Expressed this way, the value of w evolves from $w_0 + w_a$ at small a (high z) to w_0 at $z = 0$. As can be seen from the right panel of Figure 6.12, the Union2.1 SN data do not support a strong evolution of w ($w_0 = -1.02 \pm 0.12$, $w_a = 0.07 \pm 0.6$), although the constraints on w_a are weak.

The statistics of distant supernovae will improve still further in the next few years. With the planned Wide-Field Infrared Survey Telescope (WFIRST) from space, and large scale surveys from the ground such as the Dark Energy Survey which began in 2013, and the Large Synoptic Survey Telescope due to come on line towards the end of the decade, the samples of SNIa will increase by one-two orders of magnitude. The measurements from these large surveys should substantially reduce the statistical errors in the SN Hubble diagram, as well as leading to improved characterisation of the systematic errors. As the confidence contours on the determinations of $\Omega_{\Lambda,0}$, w_0 , and w_a narrow down to much smaller regions of parameter space, it is hoped that we will come closer to understanding the nature and origin of the ‘Dark Energy’.

We will return to this topic in Lecture 14.